Published by
NIGERIAN SOCIETY OF PHYSICAL SCIENCES
Available online @ https://journal.nsps.org.ng/index.php/jnsps

J. Nig. Soc. Phys. Sci. 5 (2023) 1137

Journal of the Nigerian Society of Physical Sciences

Electrohydrodynamics Convection in Dielectric Rotating Oldroydian Nanofluid in Porous Medium

Pushap Lata Sharma[a], Mohini Kapalta[a], Ashok Kumar[a], Deepak Bains[a], Sumit Gupta[b], Pankaj Thakur[c,]

[a]*Department of Mathematics & Statistics, Himachal Pradesh University, Summer Hill, Shimla, India*
[b]*Rajiv Gandhi Govt college Chaura Maidan, Shimla, India*
[c]*Faculty of Science and Technology, ICFAI University, Baddi, Solan, India*

Abstract

An electrically conducting nanofluid saturated with a uniform porous medium has been tested to determine how rotation affects thermal convection. Utilizing the Oldroydian model, which incorporates the specific effects of the electric field, Brownian motion, thermophoresis and rheological factors for the distribution of nanoparticles that are top-heavy and bottom-heavy, one may use linear stability theory to ensure stability. Analysis and graphical representation of the effects of the AC electric field Rayleigh number, Taylor number, Lewis number, modified diffusivity ratio, concentration Rayleigh number and medium porosity are provided for both bottom-heavy and top-heavy distribution.

DOI:10.46481/jnsps.2023.1231

Keywords: Convection, dielectric, electric field, nanofluid, Oldroydian, porous medium, rotation

Article History :
Received: 24 November 2022
Received in revised form: 18 January 2023
Accepted for publication: 28 January 2023
Published: 02 March 2023

Communicated by: B. J. Falaye

1. Introduction

Nanofluids are fluids that include particles with a diameter of less than 100 nm and can stay suspended in them. Choi [1] was the first to coin the term. Nanofluid is a suspension of normal nano-size particles such as metals (Al, Cu), oxides ceramics (Al_2O_3, CuO), metal carbides (SiC), nitrides and carbon nanotubes in an aqueous or non-aqueous dispersion media. Because of their unique chemical and physical features, nanofluids are now considered the next-generation heat transfer fluid. Nanofluids can be used for a variety of things, including nanocomposites, electrical cooling, bio-medicine and nanostructure production transportation because of their capabilities.

Many researchers have investigated the properties of nanofluids as well as potential application scenarios. Nanofluids are perfect for heat transfer applications since they have better thermal conductivity. Because of their superior thermal conductivity, nanofluids are perfect for transferring heat. The effects of particle size, pH and zeta potential on the thermal conductivity of nanofluids have been the subject of several investigations. In nanofluids with a low concentration of metal oxides, the addition of 4 to 5 percent metal oxides by volume results in an increase in thermal conductivity of between 10 and 20 percent. Several models have been used to estimate the thermal conductivity of nanofluids.

Email address: pankaj_thakur15@yahoo.co.in (Pankaj Thakur)

The first, which relates to the thermal conductivity of particles and fluids was created by Maxwell to ascertain the thermal conductivity of colloidal suspension which is analyzed by Nield and Kuznetsov [2]. Sheu [3] has studied the thermal instability in a porous medium layer saturated with a viscoelastic nanofluid and demonstrated that oscillatory instability is possible in both bottom-heavy and top-heavy nanoparticle distributions. The results indicate a conflict between the thermophoresis, Brownian diffusion and viscoelasticity processes, leading to oscillatory rather than stationary modes of convection. Sharma et al. [4] have investigated the onset of thermal convection in an Oldroydian nanofluid layer saturating a porous medium using a Darcy-Brinkman model revolving vertically with a uniform angular velocity. Yu and Choi [5] changed the Maxwell model by considering the influence of nanolayers on the electromagnetic field. Another appealing strategy for heat transfer development in industrial systems is the use of porous media in nanofluids.

Porous media are normally saturated, hard-open cells that are often filled with fluid to allow fluid to pass through the voids. Porous media improve heat conductivity by increasing the contact area between liquid, solid and nanofluid, hence boosting the efficiency of conventional thermal systems. Due to its use in many practical applications such as chemical reactors, heat exchangers and fluid filters, the increase in thermal conductivity of nanofluid with the use of porous media has attracted many researchers for the use of materials with high porosity in the current era for many technological problems.

Natural convection in an AC/DC electric field was studied by Jones [6] and Chen et al. [7] for electrically accelerated heat movement in fluids and its applications. Convective heat transfer through polarized dielectric liquids was studied by Stiles et al. [8]. They found that the convection pattern identified by the electric field is similar to that of the well-known Bénard cell convection. In their study of the effects of electro-thermal convection on dielectric rotating fluid, Shivakumara et al. [9] discovered that an AC electric field accelerates convection initiation and boosts heat transfer. The dielectric nanofluid may be used for instrument transformers, regulating and converter transformers and other electrical devices. Sharma et al. [10] have researched of heat convection in a dielectric rheological nanofluid layer employed an AC electric field.

A Maxwellian model was used to explain the rheology of the nanofluid and it was shown that for bottom-heavy nanoparticle distributions, the electric field and the stress relaxation parameter destabilize both stationary and oscillatory modes. Sharma et al. [11] investigation into thermosolutal convection of an elastic-viscous nanofluid in a porous medium with rotation and magnetic field led them to the conclusion that stationary convection is stabilized by the magnetic field and the Taylor number, while stationary convection is destabilized by the solutal Rayleigh number, nanoparticle Rayleigh number, thermo-nanofluid Lewis number and modified diffusivity ratio The Rivlin-Ericksen fluid issue in a Darcy-Brinkman porous medium was studied by Sharma et al. [12].

Thermosolutal convection in a porous medium and its relationship to the rotation was examined by Sharma et al. [13]. Kumar et al. [14] researched thermosolutal convection in Jeffrey nanofluid with porous medium and Sharma et al. [15] studied electrohydrodynamics convection in dielectric Oldroydian nanofluid layer in porous media. For free-free, rigid-free and rigid-rigid boundaries, Poonam et al. [16] looked into the electrohydrodynamic convection in thermal instability of Jeffrey nanofluid in porous media. Shivakumara et al. [17] investigated on the problem Darcy-Brinkman model of electrical convection in a porous dielectric fluid. Chand et al. [18] examined the convection of an electric field saturated by nanofluid in a porous medium. Ramanuja et al. [19] researched MHD SWCNT-blood nanofluid flow through porous medium in the presence of viscous dissipation and radiation effects. Akinpelu et al. [20] studied hydromagnetic double exothermic chemical reactive flow with convective cooling through a porous medium using bimolecular kinetics. This concise survey of the literature shows that research has been done on the current issue, the initiation of thermal convection.

2. Mathematical formulation of problem

An infinitely extending electrically conducting horizontal layer of an incompressible rotating non-Newtonian Oldroydian nanofluid of thickness d is taken under gravity $\boldsymbol{g}\,(0,\ 0,\ -g)$. The rotating vertical angular velocity is $\boldsymbol{\Omega}(0,0,\Omega)$. The temperatures T and volumetric fractions of nanoparticles ϕ are taken to be T_0 and ϕ_0 at $z = 0$ and T_1 and ϕ_1 at $z = d$ ($T_0 > T_1$ and $\phi_1 > \phi_0$). This dielectric nanofluid layer is dominated by a uniform vertical electric field.

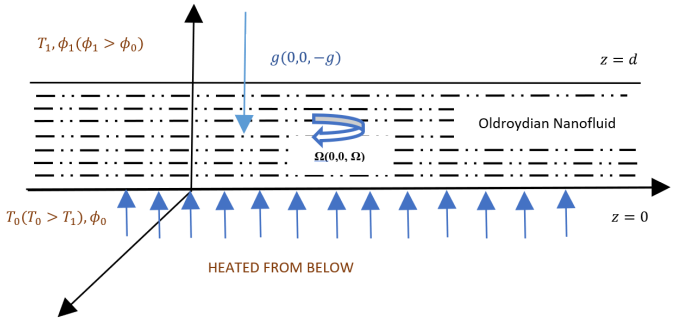

Figure 1: Physical Configuration

3. Governing equations

The conservation equations for mass and momentum using Boussinesq approximation are

$$\nabla.\boldsymbol{q_D} = 0, \tag{1}$$

$$\frac{\rho_f}{\varepsilon}\left(1+\lambda\frac{\partial}{\partial t}\right)\left[\frac{\partial}{\partial t}+\frac{1}{\varepsilon}\boldsymbol{q_D}.\nabla\right]\boldsymbol{q_D} = \left\{\begin{array}{c}\left[-\nabla p+\left(\phi\rho_p+(1-\phi)\rho_f\{1-\beta(T-T_1)\}\right)\boldsymbol{g}\right.\\ \left.+\boldsymbol{f_e}+\frac{2\rho}{\varepsilon}(\boldsymbol{\Omega}\times\boldsymbol{q_D})\right]\left(1+\lambda\frac{\partial}{\partial t}\right)-\frac{\mu}{k_1}\left(1+\lambda_0\frac{\partial}{\partial t}\right)\boldsymbol{q_D}\end{array}\right\}, \tag{2}$$

where $\boldsymbol{q_D}, p, \varepsilon, \lambda, \lambda_0, \phi, \rho_f, \rho_p, \beta, \mu$ and k_1 are the Darcy velocity, pressure, porosity, relaxation time, retardation time,

nanoparticles volume fraction, the density of the base fluid, the density of nanoparticles, coefficient of volume expansion, coefficient of viscosity and medium permeability respectively. f_e is the electrical force given by

$$\boldsymbol{f_e} = \rho_e \boldsymbol{E} - \frac{1}{2}\boldsymbol{E}^2 \nabla K + \frac{1}{2}\left(\rho \frac{\partial K}{\partial t}\boldsymbol{E}^2\right),$$

where ρ_e is the density of charge, K is the dielectric constant, $\boldsymbol{E}$ is the electric field. The term $\rho_e \boldsymbol{E}$ is due to the free charge known as Coulomb force. Here, the term $\rho_e \boldsymbol{E}$ is neglected as compared to the term $-\frac{1}{2}\boldsymbol{E}^2\nabla K$ for most dielectric fluids. The modified pressure term is

$$P = p - \frac{1}{2}\left(\rho \frac{\partial K}{\partial t}\boldsymbol{E}^2\right), \tag{3}$$

where p is the hydrodynamical pressure.

Maxwell Equations are

$$\nabla.(K\boldsymbol{E}) = 0, \nabla \times \boldsymbol{E} = 0. \tag{4}$$

From equation (4), $\boldsymbol{E}$ can be shown as

$$\boldsymbol{E} = -\nabla\varphi, \tag{5}$$

where φ is a measure of electric potential's root mean square. It is also assumed that

$$K = K_0\left[1 - \gamma\left(T - T_1\right)\right]. \tag{6}$$

$\gamma > 0$, where, $0 < \gamma\Delta T << 1$. Thus, the modified equations of motion for rotating Oldroydian nanofluid saturating a porous medium in the presence of an electric field become

$$\frac{\rho_f}{\varepsilon}\left(1 + \lambda\frac{\partial}{\partial t}\right)\left[\frac{\partial}{\partial t} + \frac{1}{\varepsilon}\boldsymbol{q_D}.\nabla\right]\boldsymbol{q_D}$$
$$= \left\{\begin{array}{c} \left(1 + \lambda\frac{\partial}{\partial t}\right)[-\nabla p + \left(\phi\rho_p + (1-\phi)\rho_f\left\{1 - \beta\left(T - T_1\right)\right\}\right)\boldsymbol{g} \\ -\frac{1}{2}\left(\boldsymbol{E}.\boldsymbol{E}\right)\nabla K + \frac{2\rho}{\varepsilon}(\boldsymbol{\Omega}\times\boldsymbol{q_D})] - \frac{\mu}{k_1}\left(1 + \lambda_0\frac{\partial}{\partial t}\right)\boldsymbol{q_D} \end{array}\right\}. \tag{7}$$

The nanoparticles' equation of continuity is

$$\left[\frac{\partial}{\partial t} + \frac{1}{\varepsilon}(\boldsymbol{q_D}.\nabla)\right]\phi = D_B\nabla^2\phi + \left(\frac{D_T}{T_1}\right)\nabla^2 T. \tag{8}$$

A porous medium's saturating nanofluid's heat-energy equation is

$$(\rho c)_m\frac{\partial T}{\partial t} + (\rho c)_f \boldsymbol{q_D}.\nabla T =$$
$$k_m\nabla^2 T + \varepsilon(\rho c)_p\left[D_B\nabla\phi.\nabla T + \left(\frac{D_T}{T_1}\right)\nabla T.\nabla T\right]. \tag{9}$$

The boundary conditions appropriate to the problem are

$$\left.\begin{array}{l} w = 0,\ \frac{\partial\varphi}{\partial z} = 0,\ T = T_0,\ \phi = \phi_0 \ \text{ at } \ z = 0 \\ w = 0,\ \frac{\partial\varphi}{\partial z} = 0,\ \ T = T_1,\ \phi = \phi_1 \ \text{ at } \ z = d \end{array}\right\}. \tag{10}$$

Using the non-dimensional variables

$$\left\{\begin{array}{c} (x^*,\ y^*,\ z^*) = \frac{(x,y,z)}{d},\ t^* = \frac{t\ \alpha_m}{\sigma\ d^2}, \boldsymbol{q_D^*} = \frac{\boldsymbol{q_D}\ d}{\alpha_m}, \\ p^* = \frac{pk_1}{\mu\alpha_m}, \phi^* = \frac{\phi-\phi_0}{\phi_1-\phi_0}, \varphi^* = \frac{\varphi}{\gamma E_0\Delta T d}, \\ T^* = \frac{T-T_1}{T_0\ -T_1}, \boldsymbol{E^*} = \frac{\boldsymbol{E}}{\gamma E_0\ \Delta T d}, K^* = \frac{K}{K_0}, \end{array}\right.$$

where $\sigma = \frac{(\rho c)_m}{(\rho c)_f}$ and $\alpha_m = \frac{k_m}{(\rho c)_f}$.

The non-dimensional forms of equations (1) and (5) - (9) are (asterisk is removed for convenience):

$$\nabla.\boldsymbol{q_D} = 0, \tag{11}$$

$$\frac{1}{V_a}\left(1 + \lambda_1\frac{\partial}{\partial t}\right)\left[\frac{1}{\sigma}\frac{\partial}{\partial t} + \frac{1}{\varepsilon}\boldsymbol{q_D}.\nabla\right]\boldsymbol{q_D} =$$
$$\left\{\begin{array}{c} \left(1 + \lambda_1\frac{\partial}{\partial t}\right)[-\nabla p - R_n\phi\hat{\boldsymbol{e}}_z - R_m\hat{\boldsymbol{e}}_z + R_aT\hat{\boldsymbol{e}}_z + R_eT\hat{\boldsymbol{e}}_z \\ -R_e\frac{\partial\varphi}{\partial z} + \sqrt{T_a}(v\hat{\boldsymbol{e}}_{\boldsymbol{x}} - u\hat{\boldsymbol{e}}_{\boldsymbol{y}})] - \left(1 + \lambda_2\frac{\partial}{\partial t}\right)\boldsymbol{q_D} \end{array}\right\}, \tag{12}$$

$$\frac{1}{\sigma}\frac{\partial\phi}{\partial t} + \frac{1}{\varepsilon}\boldsymbol{q_D}.\nabla\phi = \frac{1}{L_e}\nabla^2\phi + \frac{N_A}{L_e}\nabla^2 T, \tag{13}$$

$$\frac{\partial T}{\partial t} + \boldsymbol{q_D}.\nabla T = \nabla^2 T + \frac{N_B}{L_e}\nabla\phi.\nabla T + \frac{N_AN_B}{L_e}\nabla T.\nabla T, \tag{14}$$

$$\boldsymbol{E} = -\nabla\varphi, \tag{15}$$

$$K = \left[1 - \gamma T\left(T_0 - T_1\right)\right], \tag{16}$$

where the non-dimensional parameters are $\lambda_1 = \frac{\lambda\alpha_m}{\sigma d^2}$ is the Deborah number, $\lambda_2 = \frac{\lambda_0\alpha_m}{\sigma d^2}$ is the Strain-Retardation time parameter, $P_r = \frac{\mu}{\rho_f\ \alpha_m}$ is the Prandtl number, $D_r = \frac{k_1}{d^2}$ is the Darcy number, $V_a = \frac{\varepsilon P_r}{D_r}$ is the Vadasz number, $L_e = \frac{\alpha_m}{D_B}$ is the Lewis number, $R_a = \frac{\rho_f\ g\beta dk_1(\ T_0 - T_1)}{\mu\alpha_m}$ is the thermal Darcy-Rayleigh number, $R_m = \frac{[\phi_0\rho_p + (1-\phi_0)\rho_f\ ]gdk_1}{\mu\alpha_m}$ is the basic density Rayleigh number, $R_n = \frac{(\rho_p - \rho_f\ )(\phi_1 - \phi_0)gdk_1}{\mu\alpha_m}$ is the concentration Rayleigh number, $N_A = \frac{D_T(\ T_0 - T_1)}{D_B\ T_1\ (\phi_1 - \phi_0)}$ is the modified diffusivity ratio, $N_B = \frac{\varepsilon(\rho c)_p(\phi_1 - \phi_0)}{(\rho c)_f}$ is the modified particle-density increment, $\sqrt{T_a} = \frac{2\Omega\rho k_1}{\varepsilon\mu}$ is Taylor number and $R_e = \frac{K\gamma^2E_0^2(T_0 - T_1)^2k_1d^2}{\mu\alpha_m}$ is the AC electric Rayleigh number.

In terms of non-dimensional form, boundary conditions (10) transform to

$$\left.\begin{array}{l} w = 0,\ \frac{\partial\varphi}{\partial z} = 0,\ T = 1,\ \phi = 0\ at\ \ z = 0 \\ w = 0,\ \frac{\partial\varphi}{\partial z} = 0,\ T = 0,\ \phi = 1\ at\ \ z = 1 \end{array}\right\}. \tag{17}$$

4. Basic state solution

The basic state is stated as

$$\left\{\begin{array}{c} \boldsymbol{q_D} = (u, v, w) = (0, 0, 0),\ p = p_b(z),\ T = T_b(z), \\ \phi = \phi_b(z),\ K = K_b(z), \boldsymbol{E} = \boldsymbol{E}_b(z),\ \varphi = \varphi_b(z). \end{array}\right. \tag{18}$$

When there is no motion, equations (13) and (14) require the temperature and the volumetric fraction of nanoparticles to satisfy the equations

$$\frac{d^2\phi_b}{dz^2} + N_A\frac{d^2T_b}{dz^2} = 0, \tag{19}$$

$$\frac{d^2T_b}{dz^2} + \frac{N_B}{L_e}\frac{d\phi_b}{dz}\frac{dT_b}{dz} + \frac{N_AN_B}{L_e}\frac{dT_b}{dz}\frac{dT_b}{dz} = 0. \tag{20}$$

Using the boundary conditions (17), equation (19) can be integrated to give

$$\phi_b(z) = -N_AT_b + (1 - N_A)z + N_A. \tag{21}$$

Substituting ϕ_b from equation (21) into equation (20), we get

$$\frac{d^2T_b}{dz^2} + \frac{(1-\ N_A)N_B}{L_e}\frac{dT_b}{dz} = 0. \tag{22}$$

Equation (22) along with the boundary condition (14) gives the solution as

$$T_b = e^{-(1-\ N_A)N_Bz/L_e}\left(\frac{1-e^{-(1-N_A)N_B(1-z)/L_e}}{1-e^{-(1-N_A)N_B/L_e}}\right). \tag{23}$$

The terms of second and higher order in the expansion of an exponential function in equation (23) are neglected as they are small and so one gets the best approximate initial stationary state solutions as

$$\left\{\begin{array}{l} T_b = 1-z,\ \ \phi_b = z,\ \ K_b = 1+\gamma\Delta Tz,\ \ \boldsymbol{E}_b = \\ \frac{E_0}{\gamma\Delta T(1+\gamma\Delta Tz)},\ \ \varphi_b = -\frac{E_0}{(\gamma\Delta T)^2}\log\left(1+\gamma\Delta T\right), \end{array}\right. \tag{24}$$

where, $\boldsymbol{E}_0 = \frac{-\gamma\Delta T\varphi}{\log(1+\gamma\Delta T)}$ at $z = 0$.

5. The formulae for perturbations

By adding minute disturbances to the state variables, we can gently perturb the initial condition indicated by equation (24) so that

$$\left\{\begin{array}{c} \boldsymbol{q_D} = (0,\ 0,\ 0) + \boldsymbol{q_D'}(u',\ v',\ w'), T = T_b + T', \\ \phi = \phi_b + \phi', p = p_b + p', K = K_b + K', \\ \boldsymbol{E} = \boldsymbol{E}_b + \boldsymbol{E}', \varphi = \varphi_b + \varphi'. \end{array}\right. \tag{25}$$

Using these perturbations given by equation (25) and neglecting the terms of higher powers and products of perturbations (i.e., applying linear stability theory) in equations (11) - (16), the resulting linearized non-dimensional perturbed equations are:

$$\begin{array}{c}\left[\left(\left(1+\lambda_2\frac{\partial}{\partial t}\right)+\frac{1}{\sigma V_a}\left(1+\lambda_1\frac{\partial}{\partial t}\right)\frac{\partial}{\partial t}\right)^2\nabla^2 + T_a\left(1+\lambda_1\frac{\partial}{\partial t}\right)^2\frac{\partial^2}{\partial z^2}\right] \\ w' = \left\{\begin{array}{c}\left[\left(1+\lambda_2\frac{\partial}{\partial t}\right)+\frac{1}{\sigma V_a}\left(1+\lambda_1\frac{\partial}{\partial t}\right)\frac{\partial}{\partial t}\right]\left(1+\lambda_1\frac{\partial}{\partial t}\right) \\ \left[-R_n\nabla_H^2\phi' + (R_a+R_e)\nabla_H^2T' - R_e\nabla_H^2\frac{\partial\varphi'}{\partial z}\right]\end{array}\right\},\end{array} \tag{26}$$

$$\frac{1}{\sigma}\frac{\partial\phi'}{\partial t} + \frac{w'}{\varepsilon} = \frac{1}{L_e}\nabla^2\phi' + \frac{N_A}{L_e}\nabla^2T', \tag{27}$$

$$\tag{28}$$

$$\frac{\partial T'}{\partial z} - \nabla^2\varphi' = 0. \tag{29}$$

The boundary conditions (17) for the infinitesimal perturbations become

$$\left.\begin{array}{l} w' = 0, \frac{\partial^2w'}{\partial z^2} = 0, \frac{\partial\varphi'}{\partial z} = 0, T' = 1,\ \phi' = 0 \text{ at } z = 0 \\ w' = 0, \frac{\partial^2w'}{\partial z^2} = 0, \frac{\partial\varphi'}{\partial z} = 0, T' = 0,\ \phi' = 1 \text{ at } z = 1 \end{array}\right\}. \tag{30}$$

6. The normal mode analysis

For the system of equations (26) - (29), the analysis can be made in terms of two-dimensional periodic waves of assigned wave numbers. Thus, we assign the quantities describing the dependence on $x,\ y,\ t$ of the form

$$\exp\left(ik_xx + ik_yx + st\right),$$

where k_x and k_y are the wave numbers in x-direction and y-direction, respectively and $a^2 = k_x^2 + k_x^2$ is the resultant wave number, s is the growth rate, which is a complex constant. The above consideration allows us to suppose

$$(w', T', \phi', \varphi') = (W, \Theta, \Phi, \Psi)\exp\left(ik_xx + ik_yy + st\right). \tag{31}$$

Using expression (31), the equations (26) - (29), reduces to

$$\begin{array}{c}\left(\left((1+\lambda_2s) + \frac{1}{\sigma V_a}(1+\lambda_1s)\,s\right)^2\left(D^2-a^2\right) + T_a(1+\lambda_1s)^2D^2\right) \\ W = \left\{\begin{array}{c}\left((1+\lambda_2s)+\frac{1}{\sigma V_a}(1+\lambda_1s)\,s\right)(1+\lambda_1s) \\ \left(a^2R_n\Phi - a^2(R_a+R_e)\,\Theta + a^2R_eD\Psi\right)\end{array}\right\},\end{array} \tag{32}$$

$$\frac{s}{\sigma}\Phi + \frac{W}{\varepsilon} = \frac{1}{L_e}\left(D^2-a^2\right)\Phi + \frac{N_A}{L_e}\left(D^2-a^2\right)\Theta, \tag{33}$$

$$s\Theta - W = \left(D^2-a^2\right)\Theta + \frac{N_B}{L_e}(D\Theta - D\Phi) - \frac{2N_AN_B}{L_e}D\Theta, \tag{34}$$

$$D\Theta - \left(D^2-a^2\right)\Psi = 0, \tag{35}$$

where $a = \sqrt{k_x^2+k_y^2}$.

The equations (30) for a free-free boundary are:

$$W = D^2W = \Theta = \Phi = \ D\Psi = 0 \text{ at } z = 0 \text{ and } z = 1. \tag{36}$$

Therefore

$$\left\{\begin{array}{l} W = A_1\sin\pi z,\ \Theta = A_2\sin\pi z, \\ \Phi = A_3\sin\pi z, \Psi = A_4\cos\pi z, \end{array}\right. \tag{37}$$

where A_1, A_2, A_3 and A_4 are the constants.

Substituting (37) in equations (32) - (35) and using the boundary conditions (36), we get

$$\left[\begin{array}{cccc} \boldsymbol{A} & \boldsymbol{B} & \boldsymbol{C} & \boldsymbol{D} \\ 1 & -J-s & 0 & 0 \\ \frac{1}{\varepsilon} & \frac{N_AJ}{L_e} & \frac{J}{L_e}+\frac{s}{\sigma} & 0 \\ 0 & -\pi & 0 & -J \end{array}\right]\left[\begin{array}{c} A_1 \\ A_2 \\ A_3 \\ A_4 \end{array}\right] = \left[\begin{array}{c} 0 \\ 0 \\ 0 \\ 0 \end{array}\right], \tag{38}$$

where

$$\left\{\begin{array}{c} \boldsymbol{A} = M^2J + \pi^2T_a(1+\lambda_1s)^2, \boldsymbol{B} = -a^2(1+\lambda_1s)\,M(R_a+R_e), \\ \boldsymbol{C} = a^2(1+\lambda_1s)\,MR_n, \boldsymbol{D} = -a^2\pi(1+\lambda_1s)\,MR_e, \\ J = \left(\pi^2+a^2\right),\ \text{ and } \ M = \left((1+\lambda_2s)+\frac{1}{\sigma V_a}(1+\lambda_1s)\,s\right). \end{array}\right.$$

where, the thermal Darcy-Rayleigh number,

$$R_a = \left\{\begin{array}{c} -\frac{a^2}{\pi^2+a^2}R_e - \frac{\sigma L_e}{\sigma\left(\pi^2+a^2\right)+sL_e}\left[\frac{\pi^2+a^2+s}{\varepsilon} + \frac{\left(\pi^2+a^2\right)N_A}{L_e}\right] \\ R_n + \frac{\pi^2+a^2+s}{a^2}\left[\frac{\pi^2+a^2}{1+\lambda_1s}\left((1+\lambda_2s)+\frac{1}{\sigma V_a}(1+\lambda_1s)\,s\right)\right. \\ \left. + \frac{\sigma V_a\pi^2}{\sigma V_a(1+\lambda_2s)+(1+\lambda_1s)s}(1+\lambda_1s)\,T_a\right] \end{array}\right\}. \tag{39}$$

7. Stationary Convection

For the validity of the principle of exchange of stabilities (i.e., steady case), we have $s = 0$ ($s = r + i\omega = 0 \Rightarrow r = \omega = 0$) at the marginal stability.

Putting $s = 0$ in equation (39), we get the thermal Darcy-Rayleigh number at which marginally stable steady mode exists, as

$$R_a = \left\{ \begin{array}{c} \frac{(\pi^2+a^2)^2}{a^2} - \frac{a^2}{\pi^2+a^2} R_e - \left(\frac{L_e}{\varepsilon} + N_A\right) R_n \\ + \frac{\pi^2(\pi^2+a^2)}{a^2} T_a \end{array} \right\}, \tag{40}$$

which expresses the stationary thermal Darcy-Rayleigh number R_a as a function of the dimensionless wave number a, electric Rayleigh number R_e, Taylor number T_a, nanofluid Lewis number L_e, modified diffusivity ratio N_A, concentration Rayleigh number R_n and medium porosity ε. It is clear from the equation (40) that R_a is independent of stress relaxation time λ_1, strain retardation time λ_1 for stationary modes since these vanish with the vanishing of s (growth rate).

The minimum value of R_a is obtained by putting $\frac{\partial R_a}{\partial a^2} = 0$ and which on simplification implies that

$$\left\{ \begin{array}{c} (a_c)^8 + 2\pi^2 (a_c)^6 - \left(\pi^2 R_e + \pi^2 T_a\right)(a_c)^4 \\ -2\pi^2 (1 + T_a)(a_c)^2 - \pi^2 (1 + T_a) \end{array} \right\} = 0. \tag{41}$$

Therefore, the critical wave number a_c shows a substantial increase when the electric Rayleigh number R_e increases and is independent of nanoparticles.

To obtain the critical wave number we substitute the electric field i.e., $R_e = 0$ and we get

$$a_c{}^2 = \pi^2 \sqrt{1 + T_a}, \tag{42}$$

which is the critical wave number for stationary Rayleigh number in the absence of AC electric Rayleigh number R_e.

8. Results and discussion

To study $R_e, T_a, L_e, N_A, R_n, \varepsilon$ on the stationary convection, we examine the behavior $\frac{\partial R_a}{\partial R_e}$, $\frac{\partial R_a}{\partial T_a}$, $\frac{\partial R_a}{\partial L_e}$, $\frac{\partial R_a}{\partial N_A}$, $\frac{\partial R_a}{\partial R_n}$ and $\frac{\partial R_a}{\partial \varepsilon}$ analytically.

From equation (40) we obtain

$$\frac{\partial R_a}{\partial R_e} = -\frac{a^2}{(\pi^2 + a^2)}, \tag{43}$$

which is always negative for all wave numbers. Thus, AC electric field has destabilizing effect for both bottom-heavy and top-heavy distribution.

Equation (40) gives

$$\frac{\partial R_a}{\partial T_a} = \frac{\pi^2 \left(\pi^2 + a^2\right)}{a^2}, \tag{44}$$

which is always positive for all wave numbers. Thus, the Taylor number has stabilizing effect for both bottom-heavy and top-heavy distribution in the system.

Equation (40) further yields

$$\frac{\partial R_a}{\partial L_e} = -\frac{R_n}{\varepsilon}, \ \frac{\partial R_a}{\partial N_A} = -R_n. \tag{45}$$

It is clear from equation (45), the nanofluid Lewis number L_e and the modified diffusivity ratio N_A enhance the stationary convection if $R_n < 0$ and postpone the stationary convection if $R_n > 0$.

Equation (40) also depicts that

$$\frac{\partial R_a}{\partial R_n} = -\left(\frac{L_e}{\varepsilon} + N_A\right), \tag{46}$$

which is always negative for $\left(\frac{L_e}{\varepsilon} + N_A\right) > 0$. The nanoparticle Rayleigh number postpones the stationary convection for both bottom-heavy and top-heavy configurations.

$$\frac{\partial R_a}{\partial \varepsilon} = \frac{L_e R_n}{\varepsilon^2}. \tag{47}$$

If $R_n < 0$, thus the medium porosity delays the stationary convection for bottom-heavy configuration and if $R_n > 0$ the medium porosity advances the stationary convection.

9. Numerical discussion

The variation of thermal Darcy-Rayleigh number with respect to wave number has been plotted using equation (40) for stationary case, whereas the experimental values and the fixed permissible values of the dimensionless parameters are $R_e = 100, T_a = 100, L_e = 200$, $N_A = -5$ and $N_A = 5$, $R_n = -0.1$ and $R_n = 0.1$ and $\varepsilon = 0.6$. The stationary thermal Rayleigh number does not depend upon stress relaxation time and strain retardation time, since it vanishes with the vanishing of s (growth rate). Thus, the Oldroydian nanofluid acts like a Newtonian nanofluid.

Figures 2 and 3 show the variation of R_a for stationary convection with respect to the non-dimensional wave number for three different values of $R_e = 100,\ 300,\ 500$ for bottom-heavy and top-heavy distribution and fixed permissible values. The graph indicates that the value of R_a drops as R_e rises, indicating that R_e has a destabilizing influence on both bottom-heavy and top-heavy configurations.

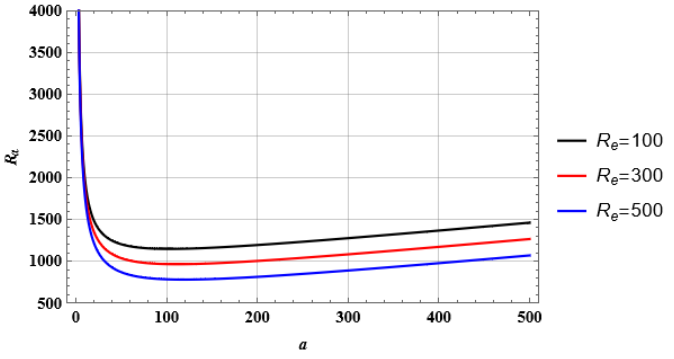

Figure 2: Variations of R_a for distinct values of the R_e for bottom-heavy distribution

Figures 4 and 5 show that R_a increases with an increase in T_a which implies that T_a has a stabilizing effect on stationary

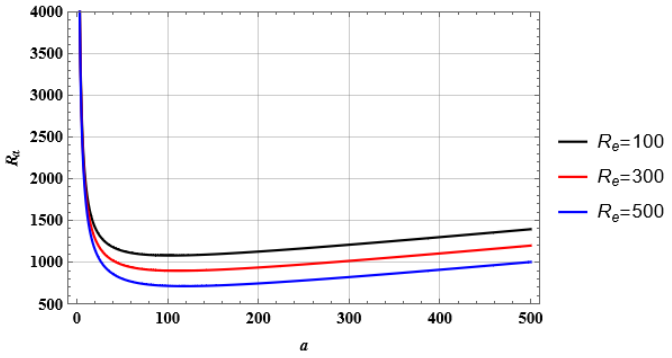

Figure 3: Variations of R_a for distinct values of R_e for top-heavy distribution

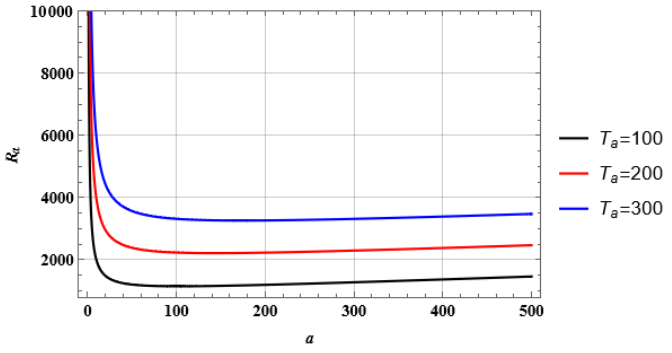

Figure 4: Variations of R_a for distinct values of T_a for bottom-heavy arrangement

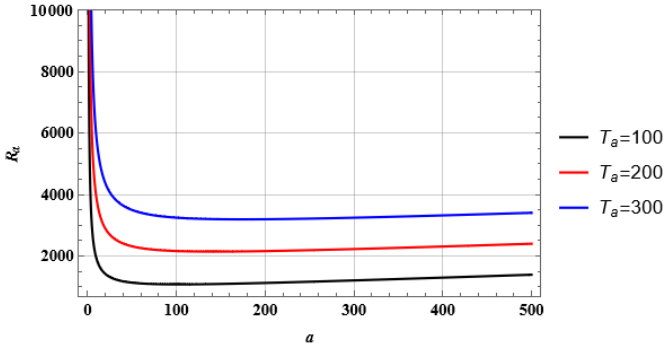

Figure 5: Variations of R_a for distinct values of T_a for top-heavy arrangement

convection for both bottom-heavy and top-heavy pattern of the system.

From figures 6 and 7, It is found from the graphs that with an increase in the values of L_e, R_a increases for bottom-heavy distribution, whereas R_a decreases for top-heavy configuration with increase in the values of the Lewis number. Hence, R_a stabilizes the bottom-heavy arrangement and destabilizes the top-heavy arrangement.

Figures 8 and 9 show that R_a increases slightly with increase in N_A for bottom-heavy arrangement and R_a decrease slightly

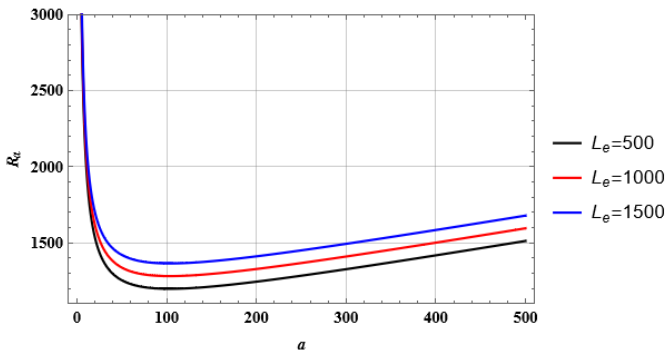

Figure 6: Variations of stationary R_a for different values of L_e for bottom-heavy distribution

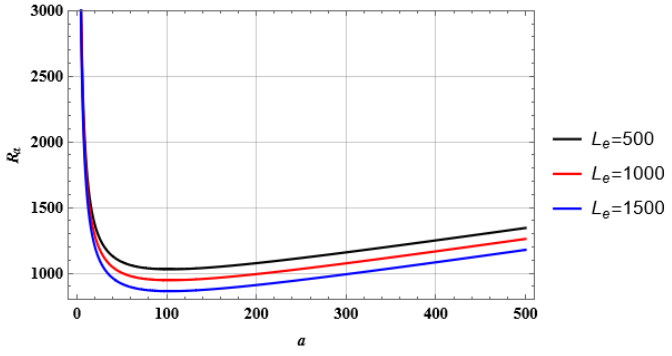

Figure 7: Variations of R_a for different values of L_e for top-heavy distribution

with increase in the modified diffusivity ratio for top-heavy arrangement. Hence N_A stabilize the system for bottom-heavy arrangement and destabilize the system for top-heavy arrangement.

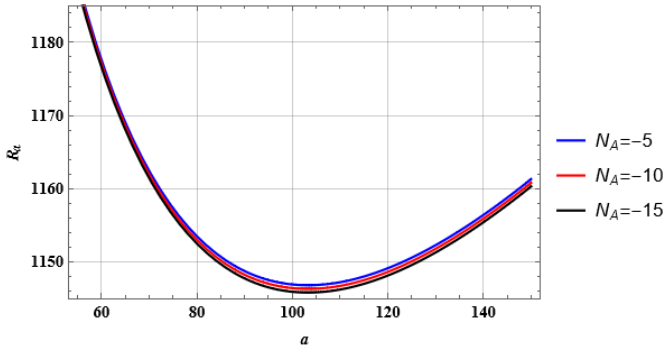

Figure 8: Variations of R_a for different values of N_A for bottom-heavy arrangement

Figures 10 and 11 show the variation of R_a for stationary convection with respect to the non-dimensional wave number for different values of R_n. It is depicted from the graphs that for the cases of bottom-heavy and top-heavy configuration, R_a decreases with the increase in R_n which causes the destabilizing

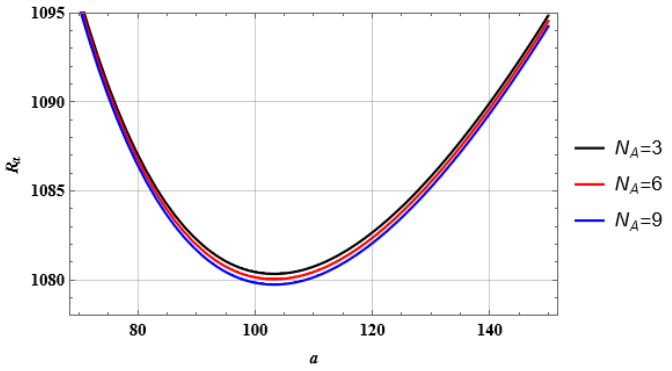

Figure 9: Variations of R_a for different values of N_A for top-heavy arrangement

effect on the system.

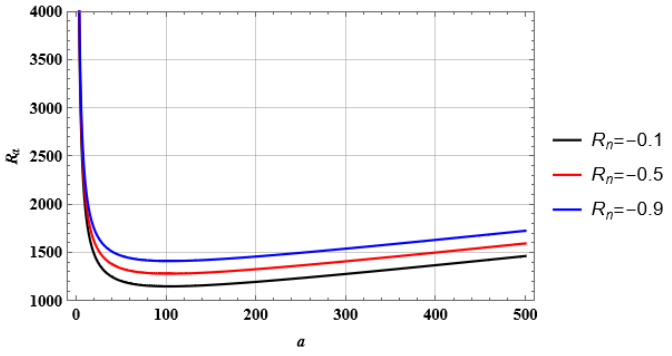

Figure 10: Variations of R_a for different values of R_n for bottom-heavy arrangement

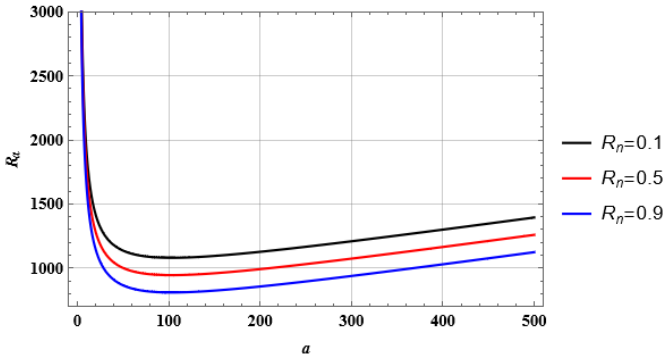

Figure 11: Variations of R_a for different values of R_n for top-heavy arrangement

The effect of the medium porosity ε on R_a is displayed in figures 12 and 13. It is found that with an increase in the ε, R_a decreases and increases, respectively for bottom-heavy and top-heavy configurations. Thus, a porous medium destabilizes the system for the bottom-heavy pattern and stabilizes the system for the top-heavy pattern.

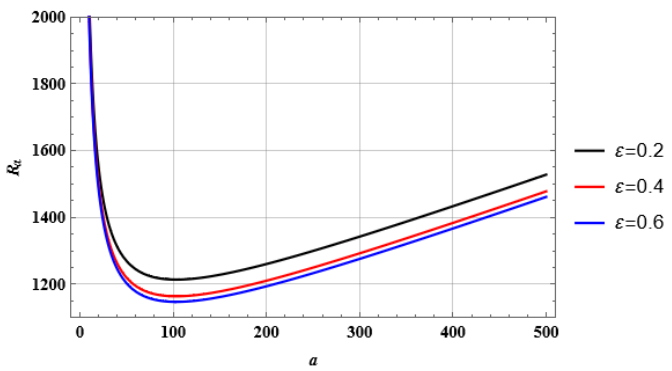

Figure 12: Variations of R_a for three different values of ε bottom-heavy distribution

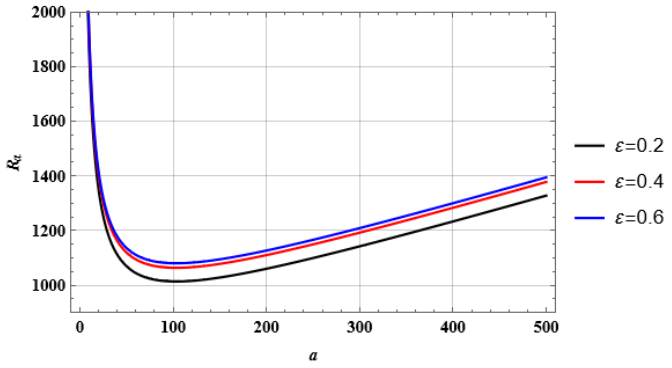

Figure 13: Variations of R_a for three different values of ε top-heavy distribution

10. Conclusions

The effect of rotation on thermal convection in an electrically conducting nanofluid saturated by porous medium has been studied using linear stability theory by employing an Oldroydian model which incorporates the effects of the electric field, Brownian motion, thermophoresis and rheological parameters for bottom-heavy and top-heavy distribution of nanoparticles. The conclusions of the present study are given below:

1. AC electric field has destabilizing for both bottom-heavy and top-heavy distribution of nanoparticles.
2. The Taylor number T_a has stabilizing for both bottom-heavy and top-heavy distribution of nanoparticles.
3. The effect of Lewis number (non-dimensional parameter accounting for Brownian motion parameter D_B) tends to stabilize the stationary convection for bottom-heavy distribution and destabilizes for top-heavy configuration.
4. Modified diffusivity ratio has stabilized the system for bottom-heavy and destabilized the system for top-heavy configuration.
5. The concentration Rayleigh number postpones the stationary convection for both bottom-heavy and top-heavy distribution.

6. Medium porosity has destabilizing effect for bottom-heavy distribution and stabilizing effect for top-heavy distribution on stationary convection.

Acknowledgments

The third author gratefully acknowledges the financial assistance of CSIR-HRDG for JRF.

References

[1] S. U. S. Choi, "Enhancing thermal conductivity of fluids with nanoparticles", Siginer, D. A., Wang, H. P. (eds.) Developments and Applications of Non-Newtonian Flows **66** (1995) 99.

[2] D. A. Nield & A. V. Kuznetsov, "The onset of convection in a horizontal nanofluid layer of finite depth", European Journal of Mechanics-B/fluids **29** (2010) 217.

[3] L. J. Sheu, "Thermal instability in a porous medium layer saturated with a viscoelastic nanofluid", Transport in Porous Media **88** (2011) 461.

[4] V. Sharma, R. Kumari & S. Garga, "Overstable convection in rotating Oldroydian nanofluid layer saturated a Darcy-Brinkman porous medium embedded by dust particle", Recent Trends in Algebra and Mechanics **18** (2014) 149.

[5] W. Yu & S. U. S. Choi, "The role of interfacial layers in the enhanced thermal conductivity of nanofluids: A renovated Maxwell model", Journal of Nanoparticle Research **5** (2003) 167.

[6] T. B. Jones, "Electrohydrodynamically enhanced heat transfer in liquids - a review", Advances in Heat Transfer **14** (1978) 107.

[7] X. Chen, J. Cheng & X. Yin, "Advances and applications of electro hydrodynamics", Chinese Science Bulletin **48** (2003) 1055.

[8] P. J. Stiles, F. Lin & P. J. Blennerhassett, Convective heat transfer through polarized dielectric liquids, Physics of Fluids, **5** (1993) 3273.

[9] I. S. Shivakumara, J. Lee, K. Vajravelu & M. Akkanagamma, "Electrothermal convection in a rotating dielectric fluid layer: Effect of velocity and temperature boundary conditions", International Journal of Heat and Mass Transfer **55** (2012) 2984.

[10] V. Sharma, A. Chowdhary & U. Gupta, "Electrothermal convection in dielectric Maxwellian nanofluid layer", Journal of Applied Fluid Mechanics**11**, (2018) 765.

[11] P. L. Sharma, Deepak & A. Kumar, "Effects of rotation and magnetic Field on thermosolutal convection in elastico-viscous Walters' (model B') nanofluid with porous medium", Stochastic Modeling & Applications **26** (2022) 21.

[12] P. L. Sharma, A. Kumar & G. C. Rana, "On the principle of exchange of stabilities in a Darcy Brinkman porous medium for a Rivlin-Ericksen fluid permeated with suspended particles using positive operator method", Stochastic Modeling & Applications, **26** (2022) 47.

[13] P. L. Sharma, Deepak, A. Kumar & P. Thakur, "Effects of rotation on thermosolutal convection in Jeffrey nanofluid with porous medium", Structural Integrity and Life (2022).

[14] A. Kumar, P. L. Sharma, Deepak & P. Thakur, "Thermosolutal convection in Jeffrey nanofluid with porous medium", Structural Integrity and Life (2022).

[15] P. L. Sharma, M. Kapalta, Deepak, A. Kumar, V. Sharma & P. Thakur, "Electrohydrodynamics convection in dielectric Oldroydian nanofluid layer in a porous medium", Structural integrity and life (2022).

[16] P. K. Gautam, G. C. Rana & H. Saxena, "Stationary convection in the electrohydrodynamics thermal instability of Jeffrey nanofluid layer saturating a porous medium: free-free, rigid-free and rigid-rigid", Journal of Porous Media **23** (2020) 1043.

[17] I. S. Shivakumara, N. Rudraiah, J. Lee & K. Hemalatha, "The onset of Darcy-Brinkman electroconvection in a dielectric fluid saturated porous layer", Transport in Porous Media **90** (2011) 509.

[18] R. Chand, G. C. Rana & D. Yadav, "Electrothermo convection in a porous medium saturated by nanofluid", Journal of Applied Fluid Mechanics **9** (2016) 1081.

[19] M. Ramanuja, J. Kavitha, A.Sudhakar & N. Radhika, "Study of MHD SWCNT-Blood Nanofluid Flow in Presence of Viscous Dissipation and Radiation Effects through Porous Medium", Journal of the Nigerian Society of Physical Sciences **5** (2023) 1054.

[20] F.O. Akinpelu, R.A. Oderinu & A.D. Ohaegbue, "Analysis of Hydromagnetic Double Exothermic Chemical Reactive Flow with Convective Cooling through a Porous Medium under Bimolecular Kinetics". Journal of the Nigerian Society of Physical Sciences **4** (2022) 130.